Pergamon

Tetrahedron 58 (2002) 2803–2811

TETRAHEDRON

Chiral recognition and chiral sensing using zinc porphyrin dimers

Takashi Hayashi,[a,*] Toshihiro Aya,[b] Masanori Nonoguchi,[b] Tadashi Mizutani,[b] Yoshio Hisaeda,[a] Susumu Kitagawa[b] and Hisanobu Ogoshi[c]

[a]*Department of Chemistry and Biochemistry, Graduate School of Engineering, Kyushu University, Fukuoka 812-8581, Japan*
[b]*Department of Synthetic Chemistry and Biological Chemistry, Graduate School of Engineering, Kyoto University, Kyoto 606-8501, Japan*
[c]*Fukui National College of Technology, Sabae 916-8507, Japan*

Received 21 December 2001; accepted 15 February 2002

Abstract—The chiral zinc porphyrin dimer linked by the (*S*)-NMe_2 or (*R*)-2,2′-dimethoxy-1,1′-binaphthyl tightly binds diamines via a zinc–nitrogen coordinated ditopic interaction. In particular, the zinc porphyrin displays excellent enantioselectivity towards Lys. The D/L selectivity is determined to be 11–12 for the lysine derivatives. The achiral zinc porphyrin dimers linked by biphenyl unit exhibit a significantly induced CD in the Soret region in the presence of chiral diamines such as lysine amides and cystine diesters, indicating that the chirality of the amino acid derivatives can be monitored upon the complexation with the achiral zinc porphyrin dimer. These results conclude that the zinc porphyrin dimers linked by rigid spacers may be good receptors to discriminate two enantiomers or monitor the absolute configuration of a diamine.

1. Introduction

The design and preparation of an artificial chiral receptor is one of the attractive objects in host–guest chemistry, since a unique model of molecular recognition for a chiral compound might be helpful for understanding the mechanism of chiral recognition processes in biological phenomena. Furthermore, over the last two decades, the understanding of the mechanisms has provided many important insights into the preparation of asymmetric catalysts for organic syntheses, the development of sensors to determine the absolute configuration, and the chromatographic separations of enantiomers. Thus, it is important to demonstrate a useful host molecule which shows enantiomeric differentiation or chiral induction sensing.[1]

It is known that porphyrin and metalloporphyrin frameworks are suitable for constructing a host molecule, because a variety of functional groups are readily fixed at the peripheral positions of the framework and physicochemical behavior of the porphyrin ring upon the addition of a guest molecule is easily monitored by several convenient spectroscopic measurements.[2] In particular, the circular dichroism (CD) of a porphyrin is a quite powerful method to detect the binding behavior when the porphyrin has chirality within the molecule or chiral environment.[3,4] These facts have encouraged us to prepare a unique functionalized chiral porphyrin which mimics the environment of the hemoprotein. The previous research projects to obtain a chiral porphyrin can be divided into two approaches: (i) attachment of chiral units to a porphyrin ring (Scheme 1(a))[5] and (ii) modification of an achiral porphyrin having C_2 molecular symmetry after introducing the achiral

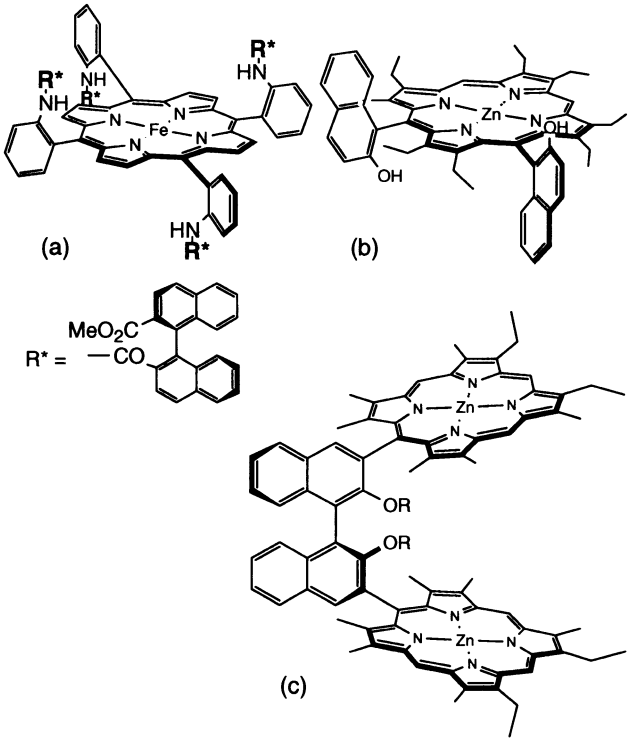

Scheme 1. Three types of chiral porphyrins.

Keywords: zinc porphyrin; porphyrin dimer; chiral recognition; chiral sensing.

* Corresponding author. Tel.: +81-92-6423595; fax: +81-92-6324718; e-mail: thayatcm@mbox.nc.kyushu-u.ac.jp

0040–4020/02/$ - see front matter
PII: S0040-4020(02)00166-7

substituents (Scheme 1(b)).[4] In fact, several groups have recently demonstrated the chiral recognition event for biologically important compounds[4,6] or enantioselective reactions[5,7] governed by 'extrinsic' or 'intrinsic' chirality within their porphyrin host molecules.

In contrast, we and several other groups have independently reported new types of chiral porphyrin molecules in which two porphyrins are linked by a chiral spacer (Scheme 1(c)).[8–11] These compounds showed a sharp induced CD band due to the exciton coupling of two porphyrin rings, so a metalloporphyrin dimer might be a good sensor for a ditopic substrate such as an α,ω-diamine.[8,9,11] In our previous paper, we have described a zinc porphyrin dimer (**1**) linked by a chiral 1,1′-binaphthyl derivative.[9] The porphyrin dimer **1** showed a size-specific interaction behavior with α,ω-diamines, $H_2N–(CH_2)_n–NH_2$, where the several alkyl lengths, n=5–10, are suitable for guest substrates. During the next stage, it has been expected that the chiral concave formed by the two metalloporphyrins leads to enantiomeric discrimination of a chiral diamine. For example, Crossley and his co-workers have recently presented the chiral recognition of histidine and lysine esters by a zinc porphyrin dimer linked by Tröger's base,[8] whereas Sessler and his co-workers have prepared several sapphyrin dimers bearing various bisamide spacers to separate the enantiomers of the aspartate and glutamate anions.[12] We have also found that each enantiomer of **1** shows some enantioselective recognition ability for a chiral substrate. However, the examples, which demonstrate the chiral recognition using porphyrin dimer linked by covalent chiral spacer, remain quite limited, although there is a variety of enantioselective separations using monomeric zinc porphyrin with intrinsic or extrinsic chirality.

An achiral zinc porphyrin dimer is also useful as a chiral sensor, since one can expect that an achiral zinc porphyrin dimer exhibits a typical CD spectrum when two porphyrin rings are fixed by binding of a chiral diamine as a guest molecule. Recently, two groups have prepared a zinc porphyrin dimer linked by a flexible alkyl chain and demonstrated that the porphyrin was a sensitive chiral sensor which suggested the absolute configuration of a chiral diamine by CD.[13,14] Furthermore, we recently found that achiral zinc porphyrin dimers **3** and **4** linked by a biphenyl spacer show very strong bisignate CD signals upon binding of chiral lysine or cystine derivatives.

This paper describe the chiral recognition and chiral sensing of amino acid derivatives using our zinc porphyrin dimers.

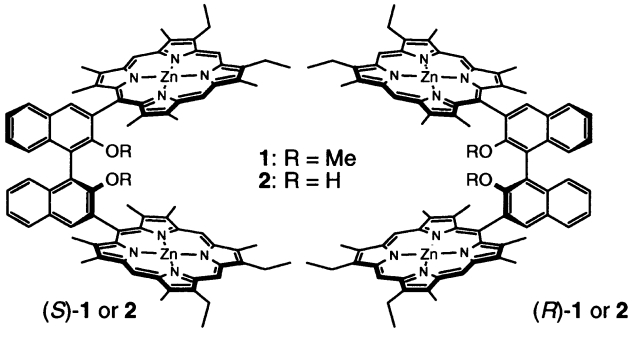

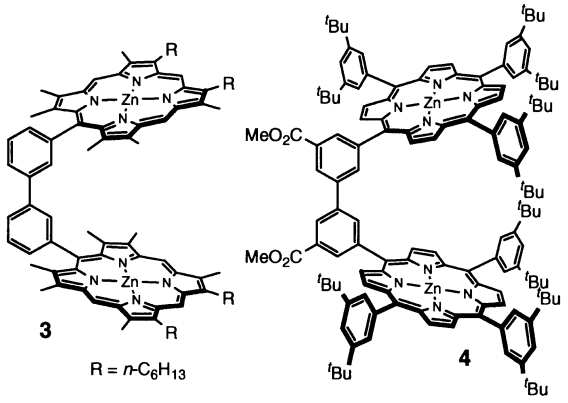

In particular, we wish to demonstrate that a relatively rigid spacer such as binaphthyl or biphenyl between two zinc porphyrin rings operates in favor of specific recognition.

2. Results and discussion

2.1. Chiral recognition

2.1.1. Ditopic interaction between chiral zinc porphyrin dimer and amino acid derivatives. To evaluate the chiral recognition ability of the porphyrin dimer concave, we have prepared a pair of enantiomers of **1**, (*S*)-**1** and (*R*)-**1**, having C_2 symmetric *S*- and *R*-binaphthol derivatives, respectively. These enantiomeric zinc porphyrin dimers were characterized by NMR, HRMS and electronic spectroscopy.[9] The chiralities of these (*S*)-**1** and (*R*)-**1** were clearly confirmed by their CD spectra, which revealed complete symmetric Cotton effects toward each other at their Soret bands.

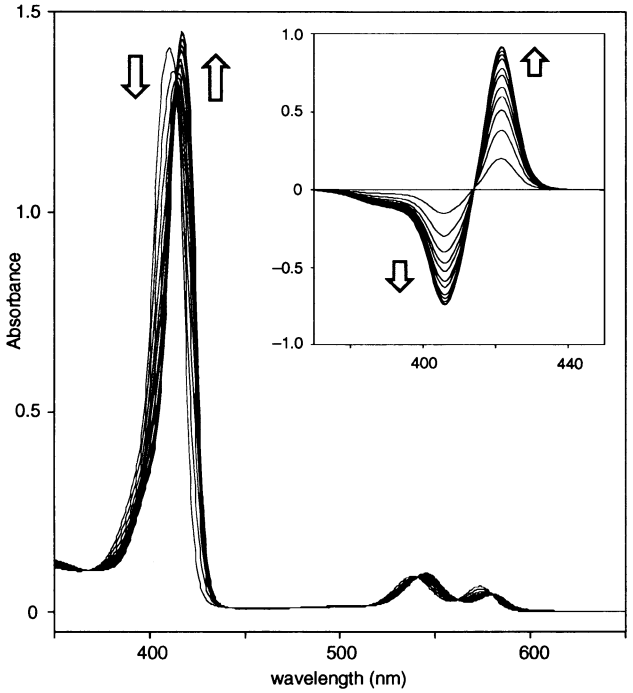

Figure 1. UV–vis titration curves for the complex between zinc porphyrin (*S*)-**1** and **5a** in CH_2Cl_2 at 15°C. Inset is the differential spectra in the Soret region. [(*S*)-**1**]=2.5 μM, [**5a**]=0–170 μM.

Table 1. Binding constants and free energy changes of (*S*)-**1** or (*R*)-**1**·amine complex formation in dichloromethane at 15°C

Host	Guest	K_a (M^{-1})[a]	$K_a(S)/K_a(R)$	$-\Delta\Delta G^\circ$ (kcal/mol)[b]
(*S*)-**1**	**5a**	160,000	12	1.4
(*R*)-**1**	**5a**	13,000		
(*S*)-**1**	**5a′**	14,000	11[c]	−1.4
(*R*)-**1**	**5a′**	150,000		
(*S*)-**1**	**5b**	120,000	8.6	1.3
(*R*)-**1**	**5b**	14,000		
(*S*)-**1**	**5c**	120,000	11	1.4
(*R*)-**1**	**5c**	11,000		
(*S*)-**1**	**6**	1,200[d]	1.2	0.1
(*R*)-**1**	**6**	980[d]		
(*S*)-**1**	1,5-Diaminopentane	180,000		

[a] Standard deviations in K_a are all within 10%.
[b] $-\Delta\Delta G^\circ = -(\Delta G^\circ_{(S)\text{-}\mathbf{1}} - \Delta G^\circ_{(R)\text{-}\mathbf{1}})$.
[c] $K_a(R)/K_a(S)$.
[d] Binding constant was determined by assuming a 1:1 complex formation between **6** and each zinc porphyrin of **1**.

Spectral changes in the Soret and Q band absorption of the zinc porphyrin dimer **1** upon the addition of the lysine derivatives **5** exhibit a 1:1 complexation with several clear isosbestic points as shown in Fig. 1. Table 1 summarizes the binding constants for the complexes of each enantiomer of **1** and **5** or leucine derivative **6**. First, compared to **6** as a chiral monoamine, chiral diamines **5a**–**5c** show significantly larger affinities for **1**. For example, the free energy change for the (*S*)-**1**·**5a** complexation is almost 1.7-fold negatively larger than that for (*S*)-**1**·**6**: $\Delta G^\circ_{(S)\text{-}\mathbf{1}\cdot\mathbf{5a}} = -6.9$ kcal/mol and $\Delta G^\circ_{(S)\text{-}\mathbf{1}\cdot\mathbf{6}} = -4.1$ kcal/mol, respectively. This result suggests that the possibility of a monotopic 1:1 complex formed by the zinc porphyrin dimer **1** and diamine **5** is ruled out under these experimental conditions. Second, Fig. 2, which shows the changes in the absorption of **1** at 421.5 nm, demonstrates the remarkable difference in affinities between (*S*)-**1**·**5a** and (*R*)-**1**·**5a**. It is found that host (*S*)-**1** exhibits a higher affinity than (*R*)-**1** for all of the guest L-amino acid derivatives **5**, indicating that the effective chiral recognition takes place by the zinc porphyrin dimer **1**. In particular, chiral dimer **1** displays excellent selectivity towards **5a**; the binding constants of (*S*)-**1** and (*R*)-**1** for **5a** are 1.6×10^5 and $1.3\times10^4\ M^{-1}$, respectively, and the difference in the free energy changes is $\Delta\Delta G^\circ_{\mathbf{1}\cdot\mathbf{5a}} = \Delta G^\circ_{(S)\text{-}\mathbf{1}\cdot\mathbf{5a}} - \Delta G^\circ_{(R)\text{-}\mathbf{1}\cdot\mathbf{5a}} = -1.4$ kcal/mol at 15°C. Furthermore, another enantiomer **5a′** shows the completely opposite binding affinity for (*S*)-**1** and (*R*)-**1**. Thus, the D/L selectivity is determined to be 11–12 for the lysine derivative. To our knowledge, the present data are some of the highest enantioselectivity values reported for artificially created chiral porphyrin systems in the recent literature.[4,6,8,12] In contrast, to the chiral monoamine, **6**, both (*S*)-**1** and (*R*)-**1** showed a much smaller affinity and almost no selectivity. These results indicate that the effective enantioselectivity results from the *ditopic* interaction in the chiral concave formed by the two zinc porphyrin rings. Interestingly, the zinc porphyrin dimer **2**, in which two methoxy groups of **1** were replaced with two hydroxyl groups, exhibited almost no enantioselectivity for **5a** ($\Delta G^\circ_{(S)\text{-}\mathbf{2}\cdot\mathbf{5a}} = \Delta G^\circ_{(R)\text{-}\mathbf{2}\cdot\mathbf{5a}} = -6.4$ kcal/mol at 15°C), although the affinity of the **2**·**5a** complex is comparable to that of the **1**·**5a** complex. Given this finding, it can be explained that the methoxy groups substituted at the chiral binaphthyl spacer amplifies the chiral environment for the porphyrin concave.

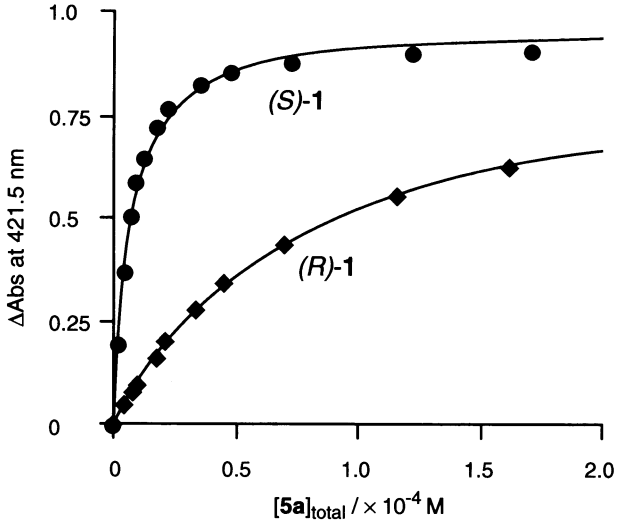

Figure 2. Plots of the absorption changes at 421.5 nm of (*S*)-**1** and (*R*)-**1** versus the total amounts of **5a** in CH_2Cl_2 at 15°C.

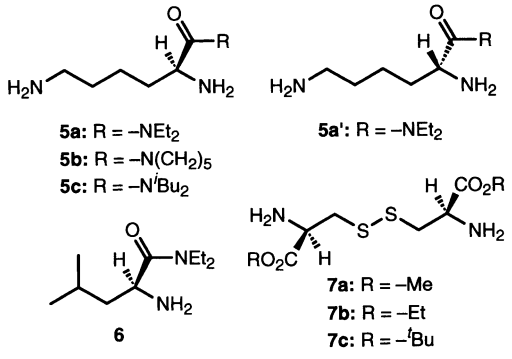

2.1.2. Estimation of plausible conformation. To analyze the experimental findings, geometry optimization for (*S*)-**1**·**5a** and (*R*)-**1**·**5a** was carried out at the semi-empirical PM3 level of theory, using the Spartan package.[†] Fig. 3 shows the optimized structure of the ditopic complexes

[†] MacSpartan Pro (version 1.0) produced by Wavefunction, Inc.

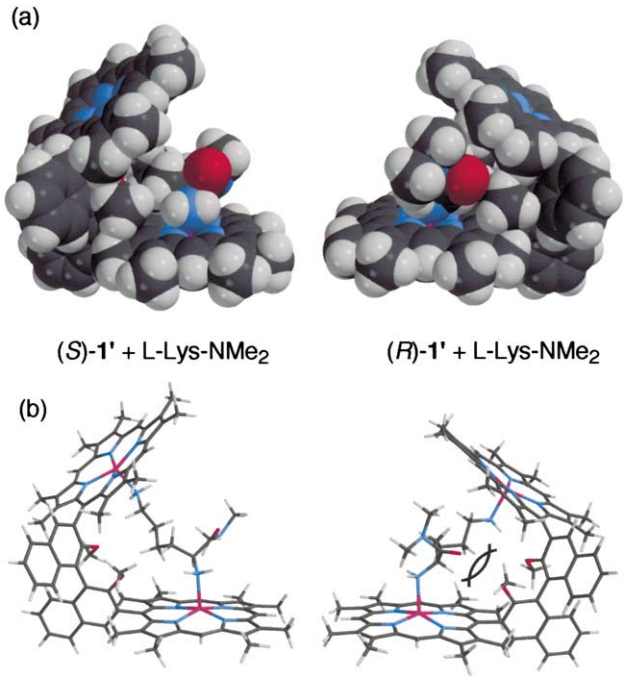

Figure 3. PM3 optimized structures of zinc porphyrin dimers (*S*)-**1**′ and (*R*)-**1**′ with L-Lys-NMe_2. (a) CPK models. (b) Stick models. Steric repulsion could have occurred in the complex between (*R*)-**1**′ and L-Lys-NMe_2.

between each enantiomer of the 1,1′-binaphthyl-2,2′-dimethoxy-3,3′-bis[(1,2,3,4,5,6,7,8-octamethylporphyrinato)zinc] (**1**′) and L-Lys-NMe_2 through zinc/nitrogen coordination. The results of the calculations suggest that the stability of the (*S*)-**1**′·L-Lys-NMe_2 complex is more favorable than that of (*R*)-**1**′·L-Lys-NMe_2. According to Fig. 3(b), it was found that steric repulsion occurs between the two

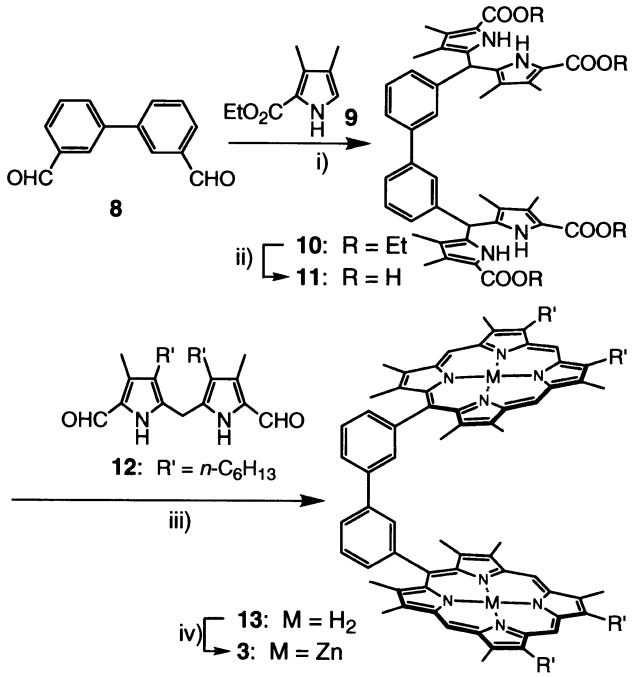

Scheme 2. Synthesis of the porphyrin dimer **3**, (i) HCl/EtOH, 90%, (ii) NaOH/EtOH, (iii) TsOH, DDQ/CH_2Cl_2–MeOH, 5.5%, (iv) $Zn(OAc)_2$/$CHCl_3$, 88%.

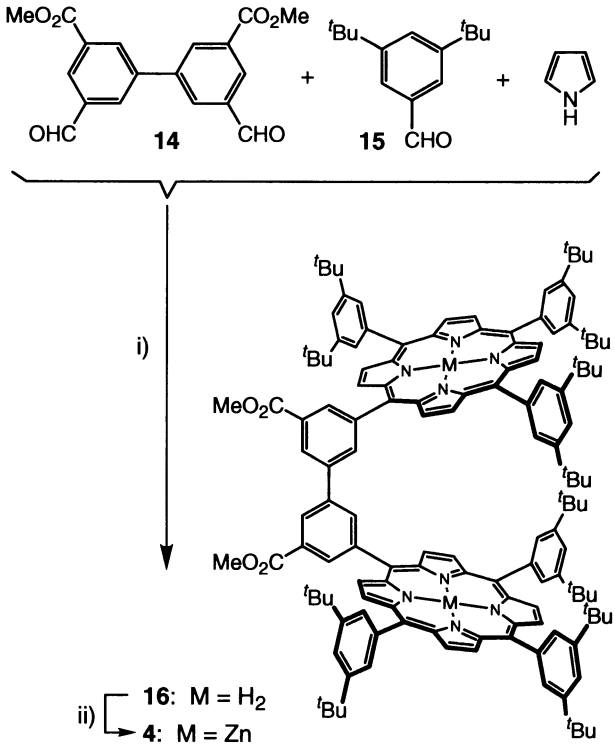

Scheme 3. Synthesis of the porphyrin dimer **4**, (i) $Zn(OAc)_2$, DDQ/$CH_3CH_2CO_2H$, 2.8 %, (ii) $Zn(OAc)_2$/CH_2Cl_2, quant.

methoxy groups of (*R*)-**1**′ and the amide group of L-Lys-NMe_2, whereas the amide group of the guest, –$CONMe_2$, in the (*S*)-**1**′·L-Lys-NMe_2 complex is oriented toward the outer space of the porphyrin dimer concave. The molecular modeling is consistent with the experimental results, in which (*S*)-**1** displays a higher affinity for **5**, indicating that the two methoxy groups of **1** play an important role in the enantiomeric differentiation of a chiral diamine guest.

2.2. Chiral sensing

2.2.1. Preparation and characterization of achiral zinc porphyrin dimers. We next focused on a zinc porphyrin dimer linked by a rotatable biphenyl spacer as a host molecule for the diamines. This is an example of a new host–guest system capable of induced-fit molecular recognition. Although the porphyrin dimer is achiral by itself and CD inactive, one can expect that a characteristic CD in the Soret region will be detected upon binding of a chiral diamine which fixes one of the twist conformations of the two porphyrin rings. Thus, according to this idea, we have designed zinc porphyrin dimers **3** and **4**. The synthetic routes for both porphyrins are shown in Schemes 2 and 3, respectively.[‡] These compounds were characterized by ^1H and ^{13}C NMR and HRMS spectroscopy.

2.2.2. Ditopic interaction between achiral porphyrin dimer and amino acid derivatives. Lysine amides **5a**–**5c** and cystine diesters **7a**–**7c** were used as the chiral diamine

[‡] The low solubility of **3** in most organic solvents prevented us from performing the NMR study. Thus, to improve the solubility of the zinc porphyrin dimer, we have also prepared **4** which has di-*tert*-butylphenyl groups at the meso position.

Table 2. Binding constants and free energy changes of **3** and **4**·amine complex formation in dichloromethane at 15°C.

Host	Guest	K_a (M^{-1})[a]	$-\Delta G°$ (kcal/mol)
3	**5a**	530,000	−7.5
3	**5b**	810,000	−7.8
3	**5c**	100,000	−6.6
3	**7a**	420,000	−7.4
3	**7b**	220,000	−7.0
3	**7c**	90,000	−6.5
4	**5c**	540,000	−7.6
4	**7a**	1,700,000	−8.2
4	**7b**	2,400,000	−8.4
4	**7c**	280,000	−7.8
3	**6**	1900	−4.2

[a] Standard deviations in K_a are all within 10%.

guests. Titrimetric measurement by UV–Vis absorption spectroscopy demonstrated a ditopic 1:1 complexation between the zinc porphyrin dimer and amino acid derivatives **5** or **7** with several isosbestic points. Table 2 depicts the binding constants of the zinc porphyrin dimer for the amino acid derivatives at 15°C in CH_2Cl_2. Compared to **3**, the zinc porphyrin dimer **4** has a relatively higher affinity for the cystine derivatives. Particularly, the binding constants of **4** for **7a** and **7b** were determined to be 1.7 and 2.4×10^6 M^{-1}, respectively. Thus, the length between the two terminal coordinated amino groups of **7a** and **7b** almost fits the Zn-to-Zn distance in the two porphyrin rings of **4**. This finding is consistent with the previous result of the size-specific interaction between the α,ω-diamine and zinc porphyrin dimer **1**.[9]

2.2.3. Structure of 4·7a complex. To estimate the structural information of the complex, we measured the ^1H NMR of the **4·7a** complex in CD_2Cl_2 at 15°C. All proton signals of **4** and **4·7a** complex were assigned by 2D-COSY and ROESY spectroscopic technique. First, the chemical shift of the methyl ester protons of guest-free **4** appeared at 3.96 ppm, whereas the addition of **7a** produced a downfield shift of the methyl protons at 4.07 ppm due to the fixation of the two porphyrin rings by the ditopic interaction of **7a**. The peaks of free **4** and complex **4·7a** were separately observed at [**7a**]/[**4**]=0.5, indicating the slow equilibrium upon complexation compared to the NMR time scale. Second, large upfield shifts of **7a** protons upon binding were observed due to the porphyrin ring current, indicating that the cystine derivative is located in the zinc porphyrin concave via ditopic interaction; The a–d protons of **7a** as shown in Fig. 4 were clearly shifted upfield by 4–5.5 ppm, however, the upfield shift of proton e of the methyl ester was lowered to approximately one-third of that observed for the other protons of **7a** (Fig. 4(a) and (b)). This finding suggests that the methyl ester of **7a** is oriented toward the outer space of the porphyrin concave. Third, the ROESY spectrum of **4·7a** exhibits remarkable cross peaks between the methyl ester protons of **7a** and two kinds of *tert*-butyl protons, and the weak cross peak between the methyl ester protons and one ortho protons of the di-*tert*-butylphenyl groups, suggesting that the methyl ester group is located between two peripheral di-*tert*-butylphenyl groups as shown in Fig. 4(c). Furthermore, the result of semi-empirical molecular orbital calculation (PM3 level)[†] indicates that the methyl ester of **7a** is close to the two

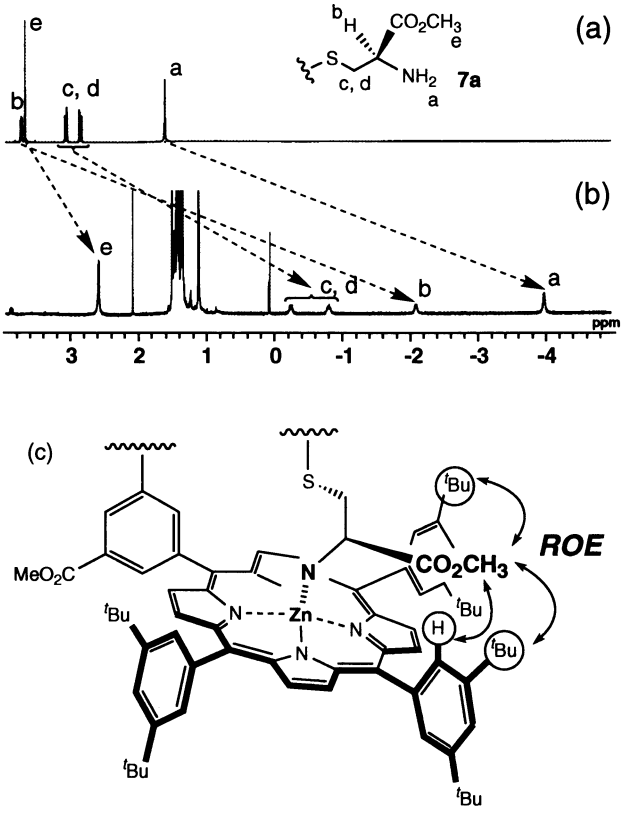

Figure 4. ^1H NMR spectra (500 MHz) of **4·7a** complex in CD_2Cl_2 at 15°C. (a) Upfield region of the 1D spectrum for **7a**. (b) The 1D spectrum for **4·7a** complex: [**4**]=[**7a**]=1 mM. (c) Estimation of molecular structure for the complex based on the results of ROESY spectrum.

tert-butyl protons of the peripheral phenyl groups, which

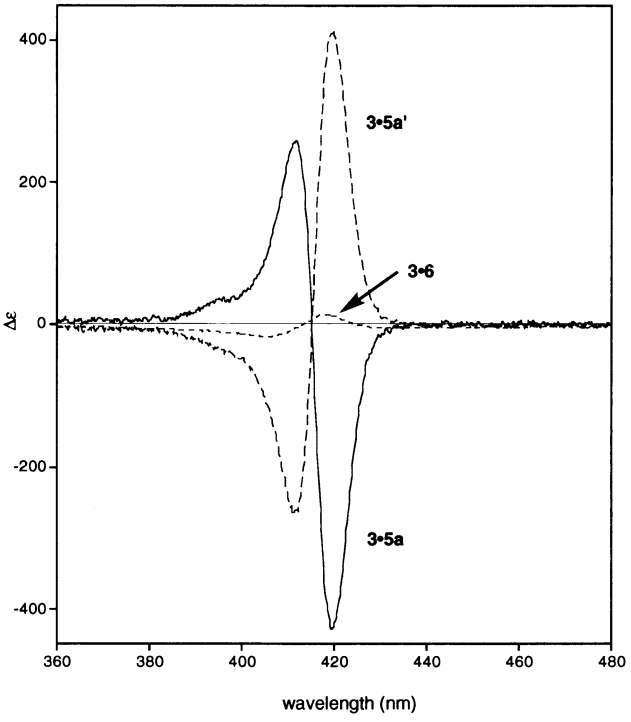

Figure 5. CD spectra of **3** and amino acid derivative complexes in CH_2Cl_2 at 15°C. Solid line, break line and dotted line represent the spectra of **3·5a**, **3·5a′** and **3·6**, respectively. [**3**]=1.6 μM, [**5a**]=[**5a′**]=18 μM, [**6**]=99 μM.

is consistent with the results of the NMR experiment (vide supra).

2.2.4. Chiral sensing monitored by CD spectroscopy. Figs. 5–7 show the CD spectra of zinc porphyrins **3** and **4** in the Soret region (360–480 nm) under the conditions where more than 95% of **3** or **4** forms the complex with guest diamines through a ditopic interaction. From the data in these figures, it can be inferred that: (i) the CD spectra of **3** and **4** in the presence of the chiral amino acid derivative **6** also give no significant signals at 15°C (Fig. 5);[14] (ii) upon the addition of amino acid derivatives **5** or **7** to the solution of the zinc porphyrin dimer, a characteristic bisignate CD band appears in the Soret region due to the exciton-coupling of the two zinc porphyrin chromophores. This finding indicates that the axial chirality of the zinc porphyrin dimers is induced by a ditopic interaction with the chiral diamine derivative; (iii) induced CD in the Soret region in the **3·5a′** complex shows a completely opposite bisignate intensity to that observed in the **3·5a** complex as shown in Fig. 5, concluding that the CD reflects the absolute configuration of the diamine; (iv) the positive CD couplet as shown in Fig. 7 suggests that the twist form of two zinc porphyrin rings in the **4·7a** complex is consistent with the result of geometry optimization of **4·7a** in which conformer of right-handed screw is the favorable structure (vide supra); (v) particularly, **3·7c** and **4·7a** reveal very sharp and strong bisignate CD with amplitude $A=+1310$ and $+957$, respectively (Figs. 6 and 7).[15,§] To our knowledge, the A values, which represent the total amplitude of the CD couplets are more than five-fold higher than those reported in the previous literature using zinc porphyrin dimers linked by a flexible spacer.[13,‖] Thus, our achiral porphyrin dimers could be suitable for a chiral sensor to sharply monitor the enantiomeric purity; and (vi) the intensity of the CD band depends on the ester substituents in a series of **5** and **7**. For **3**, the bulky *tert*-butyl ester **7c** gave the strongest coupling, whereas a significant exciton coupling was not observed in the presence of the methyl ester **7a**. In contrast, the CD of **4** exhibited a strong exciton coupling in the presence of small esters **7a** and **7b**.[¶] Given these findings, it is thought that the steric repulsion between the peripheral groups of the porphyrin and ester or amide substituent brings about the conformational variety of the porphyrin dimer–diamine adducts. Thus, the difference in the strength of the exciton coupling probably comes from the relative geometry of the

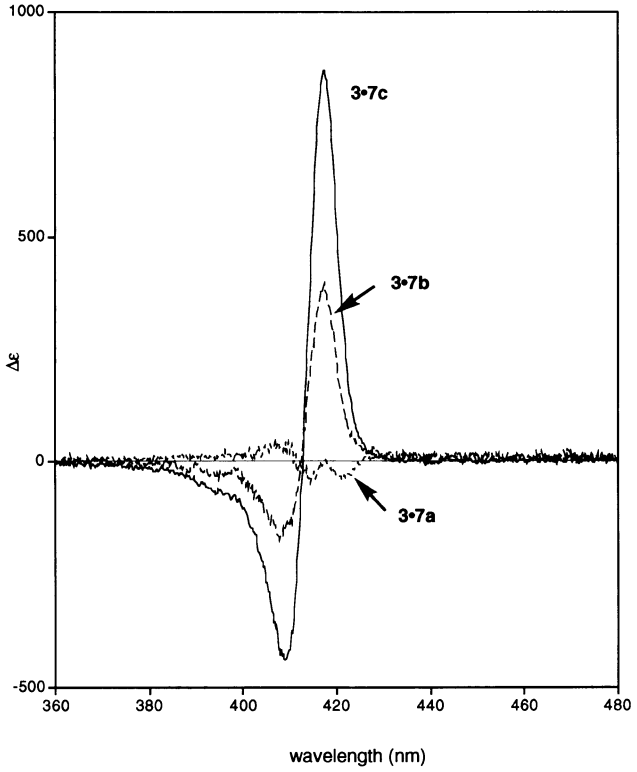

Figure 6. CD spectra of **3** and amino acid derivative complexes in CH_2Cl_2 at 15°C. Solid line, break line and dotted line represent the spectra of **3·7c**, **3·7b** and **3·7a**, respectively. [**3**]=2.1–2.3 μM, [**7a**]=150 μM, [**7b**]=72 μM, [**7c**]=190 μM.

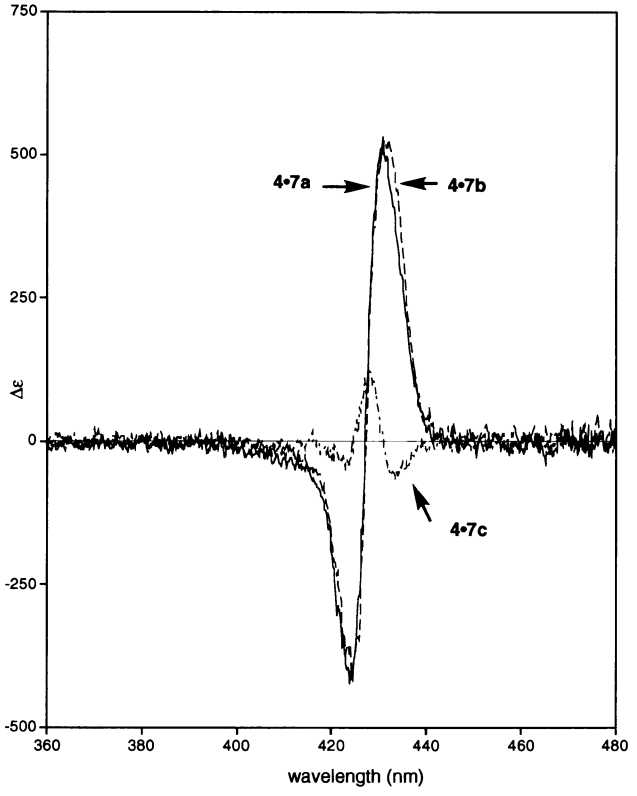

Figure 7. CD spectra of **4** and amino acid derivative complexes in CH_2Cl_2 at 15°C. Solid line, break line and dotted line represent the spectra of **4·7a**, **4·7b** and **4·7c**, respectively. No CD signals were observed in **4·6** complex. [**4**]=1.3 μM, [**7a**]=37 μM, [**7b**]=49 μM, [**7c**]=120 μM.

§ $A=\Delta\varepsilon_1-\Delta\varepsilon_2$.

‖ We also found that the intensity of the bisignate CD clearly increases with a decrease in temperature (from 15 to −45°C), although changes in the electronic absorption is less than 10%; For instance, the CD of zinc porphyrin dimer exhibited a sharp bisignate CD at −45°C with the same sign but with a >1.5-fold stronger A value of +1880 and +1280 for **3·7c** and **4·7a**, respectively. Interestingly, these findings indicate that the axial chirality of the zinc porphyrin dimers increases at lower temperature.

¶ ^{1}H NMR study suggests that one of six set of *tert*-butyl proton peaks in porphyrin dimer **4** clearly shifted upfield ($\Delta\delta=0.27$ ppm) in the presence of **7a**, since one set of *tert*-butyl groups in **4·7a** complex could be exposed to the ring current of each other zinc porphyrin inside of the concave. In contrast, only a slight upfield shift of the corresponding peaks in the **4·7c** complex ($\Delta\delta=0.12$–0.14 ppm) was observed, although **7c** is bound via a ditopic interaction. We speculate from the intensity of the bisignate CD that the twist in the two zinc porphyrin rings varies with the steric repulsion between the ester substituent and peripheral di-*tert*-butyl phenyl groups of **4**.

two chromophores upon ditopic binding of the chiral diamine.

3. Conclusion

We have demonstrated the molecular recognition of chiral diamines by zinc porphyrin dimers linked by a relatively rigid binaphthyl or biphenyl spacer for chiral diamines. First, the chiral porphyrin dimer **1** displays a prominent enantioselectivity for several lysine derivatives, indicating that the chiral concave formed by two zinc porphyrin rings effectively carries out the enantioselective discrimination for the chiral compounds. The enantioselectivity obtained in the present study is one of the best data in a series of chiral recognition systems using a chiral porphyrin as the host molecule. Second, the addition of chiral diamines to achiral zinc porphyrin dimers linked by a biphenyl spacer gives a very strong bisignate exciton coupled CD. Thus, it is concluded that our achiral porphyrin dimers having a biphenyl spacer may be quite sensitive to the chirality of some appropriate diamines. Finally, these findings indicate that the molecular concave formed by the two rigid zinc porphyrins is powerful in achieving the chiral recognition and/or chiral sensing.

4. Experimental

4.1. General procedures and methods

NMR spectra were collected on JEOL A-500 and Bruker AVANCE 500 (^{1}H: 500 MHz, ^{13}C: 125 MHz) NMR spectrometers. ^{1}H NMR chemical shift values are reported in ppm relative to the residual solvent resonances (^{1}H NMR δ 5.35 for CD_2Cl_2, δ 7.24 for $CDCl_3$, δ 7.20 for C_5D_5N and δ 4.63 for D_2O). ^{13}C NMR chemical shift values are reported in ppm relative to the solvent resonances (^{13}C NMR δ 77.0 for $CDCl_3$ and δ 123.4 for C_5D_5N). UV–Vis experiments were conducted on a Hewlett–Packard A-8452 diode array spectrophotometer with a thermostated cell compartment. Circular dichroism spectra were recorded on a JASCO J-600 spectropolarimeter with a thermostated cell compartment. Mass spectra were measured in FAB mode with a JEOL JMS-SX102 A spectrometer.

4.2. Materials

Spectrophotometric grade CH_2Cl_2 used for UV–Vis titrations was purchased from Dojindo Laboratories. $CHCl_3$ containing amylene as a stabilizer was A.C.S HPLC grade purchased from Aldrich. All organic solvents for the syntheses were dried and distilled before use. Analytical thin-layer chromatography was performed with pre-coated Merck silica gel 60, F_{254} (0.2 mm layers on glass plates). Column chromatography was performed using Merck Kiesel gel 60. The zinc porphyrin dimers **1** and **2** were prepared using previously described method. Lysine derivatives **5** were prepared by the condensation of Z-L-Lys(Z)-OH or Z-D-Lys(Z)-OH and dialkylamine in the presence of BOP reagent and subsequent deprotection. The optical purity was confirmed by the MTPA method. Leucine derivatives **6** were obtained by a procedure similar to **5**. Cystine derivatives **7** were obtained by neutralizing the L-cystine dialkyl ester dihydrochloric acids. 2-Ethoxycarbonyl-3,4-dimethylpyrrole (**9**) and 5,5′-diformyl-3,3′-di-*n*-hexyl-4,4′-dimethyldipyrrylmethane (**12**) were prepared by the usual methods. Other materials and reagents were obtained from commercial sources and used without further purification.

4.3. Data for compounds

4.3.1. 3,3′-Bis[3,3′,4,4′-tetramethyl-5,5′-bis(ethoxycarbonyl)-2,2′-dipyrrylmethyl]-1,1′-biphenyl (10). To 50 mL of EtOH containing biphenyl **8** (1.57 g, 7.47 mmol) and pyrrole **9** (5.01 g, 30.0 mmol) was added 1.2 mL of conc. HCl under a N_2 atmosphere. After reflux for 80 min, the reaction mixture was cooled. The resultant precipitate was filtered and washed with cold EtOH to yield 5.69 g (90%, 6.75 mmol) of **10**: ^{1}H NMR ($CDCl_3$) δ 8.29 (brs, 4H), 7.42 (d, J=8 Hz, 2H), 7.36 (t, J=8 Hz, 2H), 7.31 (s, 2H), 7.02 (d, J=8 Hz, 2H), 5.52 (s, 2H), 4.23 (q, J=7 Hz, 8H), 2.23 (s, 12H), 1.77 (s, 12H), 1.29 (t, J=7 Hz, 12H).

4.3.2. 3,3′-Bis(3,3′,4,4′-tetramethyl-5,5′-dicarboxy-2,2′-dipyrrylmethyl)-1,1′-biphenyl (11). To 300 mL of EtOH containing biphenyl **10** (5.14 g, 6.10 mmol) was added 5N of NaOH and the mixture was refluxed for 15 h under N_2. After removal of EtOH under reduced pressure, the residue was dissolved in H_2O and filtered. The filtrate was acidified with glacial HOAc. The resultant light purple precipitate **11** was washed with H_2O and then dried in vacuo and used without further purification: HRFAB MS calcd for $C_{50}H_{57}O_8N_4$ 841.4179 (M^+-H), found 841.4186.

4.3.3. 3,3′-Bis[13,17-dihexyl-2,3,7,8,12,18-hexamethylporphyrin-5-yl]-1,1′-biphenyl (13). To a solution of CH_2Cl_2 (630 mL) and MeOH (250 mL) containing **11** (0.908 g, 1.24 mmol) and bipyrrylmethane (**12**) (1.00 g, 2.51 mmol) was dropwise added $TsOH\cdot H_2O$ (3.74 g, 20.0 mmol) in 85 mL of MeOH over 1 h under dark condition. After stirring overnight at room temperature under N_2, the reaction mixture was exposed to the air and 2,3-dichloro-5,6-dicyano-1,4-benzoquinone (DDQ) (0.273 g, 1.20 mmol) was added and the mixture was further stirred for 2 days. After removal of the solvents under reduced pressure, the residue was dissolved in $CHCl_3$ and the solution was washed with saturated $NaHCO_3$ and H_2O. The organic layer was dried over anhydrous Na_2SO_4, and the solvent was evaporated. The main product was separated by column chromatography (silica gel, $CHCl_3$/AcOEt). The crude product was recrystallized from CH_2Cl_2/MeOH to yield 0.0840 g (5.5 %, 0.0658 mmol) of pure **13**: ^{1}H NMR ($CDCl_3$) δ 10.11 (s, 4H), 9.92 (s, 2H), 8.57 (s, 2H), 8.20 (d, J=8 Hz, 2H), 8.02 (d, J=8 Hz, 2H), 7.79 (t, J=8 Hz, 2H), 4.01 (t, J=8 Hz, 8H), 3.59 (s, 12H), 3.48 (s, 12H), 2.56 (s, 12H), 2.27 (m, 8H), 1.73 (m, 8H), 1.48 (m, 8H), 1.36 (m, 8H), 0.89 (t, J=7 Hz, 12H), −3.18 (brs, 2H), −3.34 (brs, 2H); HRFAB MS calcd for $C_{88}H_{106}N_8$ 1274.8548 (M^+), found 1274.8501.

4.3.4. Zinc porphyrin dimer (3). To 30 mL of $CHCl_3$ containing **13** (0.0277 g, 0.0217 mmol) were added five drops of saturated $Zn(OAc)_2$ in MeOH, and then the mixture was stirred overnight. After removal of the solvent under

reduced pressure, the residue was chromatographed on alumina ($CHCl_3$). The crude zinc porphyrin was recrystallized from $CHCl_3$/MeOH to yield 0.0269 g (88%, 0.0192 mmol) of pure **3**: ^{1}H NMR (C_5D_5N) δ 10.47 (s, 4H), 10.41 (s, 2H), 9.01 (s, 2H), 8.41 (d, J=8 Hz, 2H), 8.16 (d, J=7 Hz, 2H), 7.88 (t, J=8 Hz, 2H), 4.17 (t, J=8 Hz, 8H), 3.66 (s, 12H), 3.56 (s, 12H), 2.72 (s, 12H), 2.40 (m, 8H), 1.79 (m, 8H), 1.49 (m, 8H), 1.35 (m, 8H), 0.88 (t, J=7 Hz, 12H); HRFAB MS calcd for $C_{88}H_{102}N_8ZN_2$ 1398.6819 (M^+), found 1398.6846.

4.3.5. Dimethyl 3,3′-diformyl-5,5′-biphenylcarboxylate (14). Zinc powder (0.223 g, 3.41 mmol) purified with 2% HCl, $NiBr_2(PPh_3)_2$ (0.236 g, 0.318 mmol), Et_4NI (0.605 g, 2.35 mmol) and methyl 3-formyl-5-bromobenzoate (0.388 g, 1.22 mmol) were dried in vacuo. Anhydrous THF (4.0 mL) was then added and stirred at 50°C under N_2 for 22 h. After removal of the solvent, $CHCl_3$ was added to the residue and the mixture was filtered through Celite. The filtrate was washed with H_2O and the crude product was chromatographed on silica gel ($CHCl_3$/AcOEt) to yield 0.0986 g (50%, 0.302 mmol) of **14**: ^{1}H NMR ($CDCl_3$) δ 10.16 (s, 2H), 8.58 (t, J=2 Hz, 2H), 8.57 (t, J=2 Hz, 2H), 8.37 (t, J=2 Hz, 2H), 4.06 (s, 6H); HRFAB MS calcd for $C_{19}H_{14}O_6$ 326.0790 (M^+), found 326.0780.

4.3.6. 3,3′-Bis[10,15,20-tris(3,5-di-*tert*-butylphenyl)-porphyrin-5-yl]-5,5′-dimethoxycarbonyl-1,1′-biphenyl (16). Pyrrole (3.5 mL, 50.4 mmol), **14** (1.09 g, 3.34 mmol), **15** (8.84 g, 35.9 mmol) and $Zn(OAc)_2{\cdot}2H_2O$ (2.43 g, 11.1 mmol) were dissolved in 270 mL of propionic acid. The mixture was heated to 110°C for 100 min and then allowed to cool to ambient temperature. The solvents were removed under high vacuum with successive portions of toluene. To the residue, 0.993 g of DDQ in 200 mL of $CHCl_3$ was added and the mixture was stirred at room temperature with air-bubbling. After the oxidation was completed, the reaction mixture was filtered through Celite and washed with saturated $NaHCO_3$. After removal of the solvent, the residue was separated on Silica Gel column chromatography (hexane/$CHCl_3$) to collect the zinc porphyrin dimer. To remove the zinc atom, 6N HCl was poured into the $CHCl_3$ solution and the mixture was vigorously stirred for 5 min. The organic layer was collected and then washed with saturated $NaHCO_3$. The crude free base porphyrin was then purified by column chromatography on silica gel (hexane/$CHCl_3$) and recrystallized from CH_2Cl_2/MeOH to yield 0.192 g (2.9%, 0.0952 mmol) of pure **16**: ^{1}H NMR (CD_2Cl_2) δ 8.98 (t, J=2 Hz, 2H), 8.95 (t, J=2 Hz, 2H), 8.92 (t, J=2 Hz, 2H), 8.87 (br, 16H), 8.08 (t, J=2 Hz, 2H), 8.06 (t, J=2 Hz, 4H), 8.05 (t, J=2 Hz, 2H), 8.00 (t, J=2 Hz, 2H), 7.84 (t, J=2 Hz, 2H), 7.80 (t, J=2 Hz, 4H), 3.94 (s, 6H), 1.52 (s, 36H), 1.51 (s, 18H), 1.50 (s, 18H), 1.42 (s, 38H), −2.79 (s, 4H); HRFAB MS calcd for $C_{140}H_{158}N_8O_4$ 2015.2406 (M^+), found 2015.2864.

4.3.7. Zinc porphyrin dimer (4). To a solution of CH_2Cl_2 containing **16** (0.059 g, 0.0292 mmol) was added 20 drops of saturated $Zn(OAc)_2$ solution in MeOH. The mixture was stirred at room temperature for 2 h and passed through basic alumina to yield 0.0623 g (quant.) of **4**. The zinc porphyrin dimer was further purified by recrystallization from CH_2Cl_2/MeOH: ^{1}H NMR (CD_2Cl_2) δ 8.99 (t, J=2 Hz, 2H), 8.97–8.94 (m, 18H), 8.91 (t, J=2 Hz, 2H), 8.08 (t, J=2 Hz, 2H), 8.05 (t, J=2 Hz, 4H), 8.04 (t, J=2 Hz, 2H), 7.99 (t, J=2 Hz, 4H), 7.82 (t, J=2 Hz, 2H), 7.79 (t, J=2 Hz, 4H), 3.94 (s, 6H), 1.52 (s, 18H), 1.51 (s, 18H), 1.50 (s, 36H), 1.42 (s, 38H); ^{13}C NMR (CD_2Cl_2) δ 167.4, 150.9, 150.8, 150.8, 150.1, 149.1, 149.1, 144.6, 142.1, 142.0, 139.0, 137.2, 134.3, 132.9, 132.5, 131.7, 130.0, 128.0, 123.1, 122.9, 121.4, 119.1, 52.64, 35.29, 35.23, 31.81, 31.76; HRFAB MS calcd for $C_{140}H_{154}N_8O_4ZN_2$ 2139.0676 (M^+), found 2139.0811.

4.4. Binding studies

Initially, a porphyrin solution (2.0 mL, [zinc porphyrin dimer]=10^{-6} M) was poured into a 1 cm quartz cell. The UV–Vis spectrum of the pure host solution was recorded, and some of the stock guest solution (e.g. 10 μL) was transferred into the cell with a syringe. The spectrum was recorded and the process was repeated until the desired guest-to-host ratio was obtained. The parameters from the changes in the monitored absorbance were calculated using a nonlinear curve-fitting procedure based on the damped Gauss–Newton method.

Acknowledgements

This work was supported by a Grant-in-Aid for Scientific Research from the Ministry of Education, Science and Culture, Japan.

References

1. Lehn, J.-M. *Supramolecular Chemistry*; VCH: Weinheim, 1995.
2. (a) Hayashi, T.; Ogoshi, H. *Chem. Soc. Rev.* **1997**, *26*, 355–364. (b) Ogoshi, H.; Mizutani, T. *Acc. Chem. Res.* **1998**, *31*, 81–89. (c) Ogoshi, H.; Mizutani, T.; Hayashi, T.; Kuroda, Y. *The Porphyrin Handbook*; Kadish, K. M., Smith, K. M., Guilard, R., Eds.; Academic Press (San Diego) 2000; Vol. 6 Chapter 6.
3. Hsu, M.-C.; Woody, R. W. *J. Am. Chem. Soc.* **1971**, *93*, 3515–3525.
4. (a) Ogoshi, H.; Saita, K.; Sakurai, K.; Watanabe, T.; Toi, H.; Aoyama, Y.; Okamoto, Y. *Tetrahedron Lett.* **1986**, *27*, 6365–6368. (b) Aoyama, Y.; Saita, K.; Toi, H.; Ogoshi, H.; Okamoto, Y. *Tetrahedron Lett.* **1987**, *28*, 4853–4856.
5. Groves, J. T.; Myers, R. S. *J. Am. Chem. Soc.* **1983**, *105*, 5791–5796.
6. (a) Aoyama, Y.; Uzawa, T.; Saita, K.; Tanaka, Y.; Toi, H.; Ogoshi, H.; Okamoto, Y. *Tetrahedron Lett.* **1988**, *29*, 5271–5274. (b) Boitrel, B.; Lecas, A.; Rose, E. *Tetrahedron Lett.* **1988**, *29*, 5653–5655. (c) Konishi, K.; Yahara, K.; Toshishige, H.; Aisa, T.; Inoue, S. *J. Am. Chem. Soc.* **1994**, *116*, 1337–1344. (d) Mizutani, T.; Ema, T.; Tomita, T.; Kuroda, Y.; Ogoshi, H. *J. Am. Chem. Soc.* **1994**, *116*, 4240–4250. (e) Mizutani, T.; Ema, T.; Yoshida, T.; Renné, T.; Ogoshi, H. *Inorg. Chem.* **1994**, *33*, 3558–3566. (f) Kuroda, Y.; Kato, Y.; Higashioji, T.; Hasegawa, J.; Kawanami, S.; Takahashi, M.; Shiraishi, N.; Tanabe, K.; Ogoshi, H. *J. Am. Chem. Soc.* **1995**, *117*, 10950–10958. (g) Bonar-Law, R. P. *J. Am. Chem. Soc.* **1995**, *117*, 12397–12407. (h) Konishi, K.; Kimata, S.;

Yoshida, K.; Tanaka, M.; Aida, T. *Angew. Chem. Int. Ed. Engl.* **1996**, *35*, 2823–2825. (i) Mazzanti, M.; Veyrat, M.; Ramasseul, R.; Marchon, J.-C.; Turowska-Tyrk, I.; Shang, M.; Scheidt, W. R. *Inorg. Chem.* **1996**, *35*, 3733–3734. (j) Morice, C.; Maux, P. L.; Simonneaux, G.; Toupet, L. *J. Chem. Soc., Dalton Trans.* **1998**, 4165–4171. (k) Simonato, J.-P.; Pécaut, J.; Marchon, J.-C. *J. Am. Chem. Soc.* **1998**, *120*, 7363–7364. (l) Galardon, E.; Lukas, M.; Le Maux, P.; Simonneaux, G. *Tetrahedron Lett.* **1999**, *40*, 2753–2756. Galardon, E.; Le Maux, P.; Bondon, A.; Simonneaux, G. *Tetrahedron: Asymmetry* **1999**, *10*, 4203–4210.

7. (a) Mansuy, D.; Battioni, P.; Renaud, J. P.; Guerin, P. *J. Chem. Soc., Chem. Commun.* **1985**, 155–156. (b) Naruta, Y.; Tani, F.; Maruyama, K. *Chem. Lett.* **1989**, 1269–1272. (c) O'Malley, S.; Kodadek, T. *J. Am. Chem. Soc.* **1989**, *111*, 9116–9117. (d) Ohkubo, K.; Sagawa, T.; Kuwata, M.; Hata, T.; Ishida, H. *J. Chem. Soc., Chem. Commun.* **1989**, 352–354. (e) Le Maux, P.; Bahri, H.; Simonneaux, G. *J. Chem. Soc., Chem. Commun.* **1991**, 1350–1352. (f) Naruta, Y.; Tani, F.; Ishihara, N.; Maruyama, K. *J. Am. Chem. Soc.* **1991**, *113*, 6865–6872. (g) Maxwell, J. L.; O'Malley, S.; Brown, K. C.; Kodadek, T. *Organometallics* **1992**, *11*, 645–652. (h) Chiang, L.-C.; Konishi, K.; Aida, T.; Inoue, S. *J. Chem. Soc., Chem. Commun.* **1992**, 254–256. (i) Ohkubo, K.; Sagawa, T.; Ishida, H. *Inorg. Chem.* **1992**, *31*, 2682–2688. (j) Vilain, S.; Maillard, P.; Momenteau, M. *J. Chem. Soc., Chem. Commun.* **1994**, 1697–1698. (k) Collman, J. P.; Lee, V. J.; Kellen-Yuen, C. J.; Zhang, X.; Ibers, J. A.; Brauman, J. I. *J. Am. Chem. Soc.* **1995**, *117*, 692–703. (l) Le Maux, P.; Bahri, H.; Simonneaux, G.; Toupet, L. *Inorg. Chem.* **1995**, *34*, 4691–4697. (m) Rose, E.; Soleilhavoup, M.; Christ-Tommasion, L.; Moreau, G.; Collman, J. P.; Quelquejeu, M.; Straumanis, A. *J. Org. Chem.* **1998**, *63*, 2042–2044. (n) Lai, T.-S.; Kwong, H.-L.; Zhang, R.; Che, C.-M. *J. Chem. Soc., Dalton Trans.* **1998**, 3559–3564. (o) Zhou, X.-G.; Yu, X.-Q.; Huang, J.-S.; Che, C.-M. *Chem. Commun.* **1999**, 2377–2378.
8. (a) Crossley, M. J.; Hambley, T. W.; Mackay, L. G.; Try, A. C.; Walton, R. *J. Chem. Soc., Chem. Commun.* **1995**, 1077–1079. (b) Crossley, M. J.; Mackay, L. G.; Try, A. C. *J. Chem. Soc., Chem. Commun.* **1995**, 1925–1927. (c) Allen, P. R.; Reek, J. N. H.; Try, A. C.; Crossley, M. J. *Tetrahedron: Asymmetry* **1997**, *8*, 11161–11164.
9. Hayashi, T.; Nonoguchi, M.; Aya, T.; Ogoshi, H. *Tetrahedron Lett.* **1997**, *38*, 1603–1606.
10. (a) Matile, S.; Berova, N.; Nakanishi, K. *J. Am. Chem. Soc.* **1995**, *117*, 7021–7022. (b) Matile, S.; Berova, N.; Nakanishi, K.; Fleishhauer, J.; Woody, R. W. *J. Am. Chem. Soc.* **1996**, *118*, 5198–5206.
11. (a) Ema, T.; Nemugaki, S.; Tsuboi, S.; Utaka, M. *Tetrahedron Lett.* **1995**, *36*, 5905–5908. (b) Takeuchi, M.; Chin, Y.; Imada, T.; Shinkai, S. *J. Chem. Soc., Chem. Commun.* **1996**, 1867–1868. (c) Ema, T.; Misawa, S.; Nemugaki, S.; Sakai, T.; Utaka, M. *Chem. Lett.* **1997**, 487–488.
12. Sessler, J. L.; Andrievsky, A.; Král, V.; Lynch, V. *J. Am. Chem. Soc.* **1997**, *119*, 9385–9392.
13. (a) Huang, X.; Rickman, B. H.; Borhan, B.; Berova, N.; Nakanishi, K. *J. Am. Chem. Soc.* **1998**, *120*, 6185–6186. (b) Kurtán, T.; Nesnas, N.; Li, Y.-Q.; Huang, X.; Nakanishi, K.; Berova, N. *J. Am. Chem. Soc.* **2001**, *123*, 5962–5973. (c) Kurtán, T.; Nesnas, N.; Koehn, F. E.; Li, Y.-Q.; Nakanishi, K.; Berova, N. *J. Am. Chem. Soc.* **2001**, *123*, 5974–5982.
14. (a) Borovkov, V. V.; Lintuluoto, J. M.; Fujiki, M.; Inoue, Y. *J. Am. Chem. Soc.* **2000**, *122*, 4403–4407. (b) Borovkov, V. V.; Lintuluoto, J. M.; Inoue, Y. *Org. Lett.* **2000**, *2*, 1565–1568. (c) Borovkov, V. V.; Lintuluoto, J. M.; Inoue, Y. *J. Phys. Chem. A* **2000**, *104*, 9213–9219. (d) Borovkov, V. V.; Lintuluoto, J. M.; Inoue, Y. *J. Am. Chem. Soc.* **2001**, *123*, 2979–2989.
15. Harada, N.; Nakanishi, K. *Circular Dichroic Spectroscopy-Exciton Coupling in Organic Stereochemistry*; University Science Books: Mill Valley, 1983.